Chapter 2 Visible light-sensitive polymerizable and polymeric triazine-based photoinitiators with enhanced migration stability

2.1 Preface

Photopolymerization has emerged as a powerful tool for the fabrication of polymeric materials owing to its rapid reaction rate, mild conditions, and spatiotemporal control. However, increasing awareness of health and environmental issues has drawn attention to the leachability of photoinitiators (PIs) from cured networks. The migration of low-molecular-weight PIs not only compromises the long-term stability of polymeric materials but also poses potential risks in biomedical and food-packaging applications. To address this challenge, the development of polymerizable or polymeric PIs that can be covalently integrated into the polymer matrix is of growing importance.

This chapter focuses on the design and evaluation of a methacrylate-functionalized triazine-based visible light photoinitiator, 2-(((4-(2-(4,6-bis(trichloromethyl)-1,3,5-triazin-2-yl)vinyl)phenoxy)carbonyl)amino)ethyl methacrylate (CT), and its polymeric analogue (pCT) prepared via reversible addition–fragmentation chain-transfer (RAFT) polymerization. Both CT and pCT were developed to exhibit minimal migration tendency. Their photophysical properties, photolysis behavior, and photoinitiation performance were systematically investigated under violet LED irradiation (400–410 nm).

Experimental results revealed that pCT exhibited slightly reduced photoinitiation efficiency compared to CT due to steric effects, yet both demonstrated significantly improved migration resistance relative to benchmark triazine initiators MT and PT. In particular, photopolymers prepared under LED@400 and 410 nm using CT and pCT

showed only one-third to one-fourteenth of the leachability observed for reference systems.

Overall, this study demonstrates a rational strategy for designing polymerizable and polymeric triazine photoinitiators with excellent visible light reactivity and outstanding migration stability. The findings provide valuable insight into developing low-migration photoinitiator systems for safer and more durable photopolymerized materials.

2.2 Statement of contribution

I declare that the research results presented in this chapter are my original work, conducted as part of my Ph.D. program at the Australian National University.

As the first author, I was responsible for developing the research concept, designing the experimental framework, performing data analysis, preparing figures, and drafting the original manuscript, under the supervision of my primary supervisor, Professor Pu Xiao.

2.3 Publication status

The published manuscript entitled “Visible-light-sensitive polymerizable and polymeric triazine-based photoinitiators with enhanced migration stability” and the supporting information are reproduced as a chapter with permission, Copyright 2022, MDPI journals.[1] This manuscript has been published in the journal **Catalysts** in 2022, and the citation of this published manuscript is:

Li, L.; Zhu, D.; Peng, X.; Xiao, P. Visible-Light-Sensitive Polymerizable and Polymeric Triazine-Based Photoinitiators with Enhanced Migration Stability. *Catalysts* **2022**, *12*, 1305. https://doi.org/10.3390/catal12111305

2.4 Abstract

Photopolymerization has attracted great interest because of its mild reaction conditions, spatiotemporal controllability, cost-efficiency, and fast speed. However, with the raising environmental awareness and the increasing attention to life and health, the leachability of photoinitiators has become a growing concern. In this research, a methacrylate functionalized triazine based polymerizable visible light photoinitiator, 2-(((4-(2-(4,6-bis(trichloromethyl)-1,3,5-triazin-2-yl)vinyl)phenoxy)carbonyl)amino)ethyl methacrylate (CT) and its RAFT polymerized CT (pCT) were designed as the polymerizable and polymeric photoinitiators, respectively. The photoinitiation abilities of the investigated triazine derivatives were evaluated under violet LEDs. Due to the steric effect, pCT showed slightly reduced photoinitiation ability under both LED@400 and 410 nm irradiation. Nevertheless, photopolymers initiated using CT and pCT showed excellent migration stability compared to those prepared by 2-(4-methoxystyryl)-4,6-bis(trichloromethyl)- 1,3,5-triazine (MT) and 4-(2-(4,6-bis(trichloromethyl)-1,3,5-triazin-2-yl)vinyl)phenol (PT). Specifically, CT and pCT-based polymers prepared under the irradiation of LED@400 nm exhibited only 1/3-fold and 1/14-fold of photoinitiators leachability, while 1/2-fold and 1/6-fold of photoinitiator leachability were obtained compared to the MT-based photocured polymers when using LED@410 nm. The excellent migration stability of pCT has revealed the potential applications in biomedical and food packaging fields.

2.5 Introduction

Photopolymerization has been prevalent in various fields including 3D printing, coating, optoelectronics, dentistry, adhesive, and paints[2-9] due to its mild reaction conditions, spatiotemporal controllability, cost-efficiency, and high efficiency.[10-12] Many photocatalysts[13-15] and photoinitiators[16, 17] are commercially available or have been developed to initiate photopolymerization. One of the most growing concerns in photopolymerization is the migration and leachability of photoinitiators from the

photocured products. Although only a small amount of photocatalysts or photoinitiators is required in photopolymerization, unconsumed photoinitiators and their photolysis fragments still remain in the photocured products, while it is even more significant for photocatalysts as they are almost not consumed at all and remain unchanged after reactions.[18-21] The residual photocatalysts or photoinitiators and fragments produced from the photolysis of photoinitiating systems can bring undesired properties of the polymers and cause migration problems. All these issues greatly limit the applications of the produced polymers on food packaging or biochemical materials due to toxicity.[19, 22-29] Thus, the strategies to minimize the migration of photoinitiators have attracted much interest. One prevalent strategy is to introduce polymerizable groups like methacrylate group into photoinitiators, including thioxanthone, naphthalimide, and (2E,5E)-2,5-bis(4-((2-hydroxyethyl)(methyl)amino)benzylidene)cyclopentanone. This allows the crosslinking of photoinitiators into the prepared photopolymer networks, which significantly decreases their mobility. [18, 19, 29-35] Another strategy is to develop the macromolecular photoinitiators from the low molecular weight photoinitiators including bisacylphosphine oxide (BAPO), 1-hydroxy-cyclohexyl-phenylketone (HCAP), 2-hydroxy-2-methyl-1-phenyl propanone (HMPP), and naphthalimide derivatives,[36-39] and the developed macromolecular photoinitiators were well-known for their low leachability.[37-44] However, most of them only contain a low content of photoinitiator and thus require high mass concentrations.[36-42, 44] Alternatively, these polymeric photoinitiators work efficiently mainly under UV light irradiation, which limits their potential applications in household usage and making thick samples due to the potential harm of UV light to the human body and its poor penetration depth.[45-51] The most direct approach to solving these issues is to employ photoinitiators that are sensitive to longer wavelengths instead. In fact, there have been some visible light-sensitive macromolecular photoinitiators being reported.[36, 52] Specifically, a waterborne poly(ethylene glycol) substituted BAPO derivative (PEG-BAPO) was synthesized and showed a possibility of applying it in 3D printing under 460 nm LED irradiation.[36] However, it also showed a prolonged induction time of 12 s when photopolymerized only 50 um-thick samples, which could be ascribed to the

extremely low molar extinction coefficient at 460 nm. Alternatively, a series of BAPO salts and monoacylphosphineoxide (MAPO) salts were also synthesized and investigated under visible light irradiation.[52] Nevertheless, their low molar extinction coefficients under visible light range significantly affect their efficiency. Therefore, it is desirable and urgent to design and develop highly efficient visible light-sensitive photoinitiators with high migration stability for photopolymerization. 2-(4-methoxystyryl)-4,6-bis(trichloromethyl)- 1,3,5-triazine (MT) has been reported as a highly efficient photoinitiator under visible light irradiation.[45] Compared to the commercially available photoinitiators like BAPO, 2,4,6-trimethylbenzoyl diphenyl-phosphineoxide (TPO), and 2-benzyl-2-dimethylamino-1-(4-morpholinophenyl)-butanone-1 (BDMB), MT exhibits higher photoinitiation ability under the irradiation of LED@405 nm in free radical polymerization (FRP) and has been applied in 3D printing.[53] Moreover, MT, when combined with an iodonium salt and N-vinylcarbazole, can photoinitiate cationic polymerization of 3,4-epoxycyclohexylmethyl 3,4-epoxycyclohexane carboxylate (EPOX).[45] However, most photoinitiators including MT show poor cytocompatibility,[54-56] therefore, the investigation of the migration of photoinitiators after photopolymerization becomes significant.

Herein, we reported a polymerizable MT derivative and a polymeric MT derivative with high efficiency and migration stability. Specifically, the polymerizable MT derivative, 2-(((4-(2-(4,6-bis(trichloromethyl)-1,3,5-triazin-2-yl)vinyl)phenoxy)carbonyl)amino)ethyl methacrylate (CT) was synthesized by first forming 4-(2-(4,6-bis(trichloromethyl)-1,3,5-triazin-2-yl)vinyl)phenol (PT) by the demethylation of MT, followed by the coupling of PT with 2-isocyanatoethyl methacrylate. Subsequently, CT underwent RAFT polymerization to generate polymerized CT (pCT), a polymeric photoinitiator with high triazine content, as shown in Scheme 2.1. The light absorption properties of the synthesized triazine derivatives were fully studied. The photoinitiation abilities of these triazine-derivatives were investigated under the irradiation of LED@400 nm and 410 nm by the photopolymerization of trimethylolpropane triacrylate (TMPTA) via real-time Fourier-

transform infrared spectroscopy (RT-FTIR). Furthermore, the migration stability of the residual photoinitiators from photocured samples was discussed.

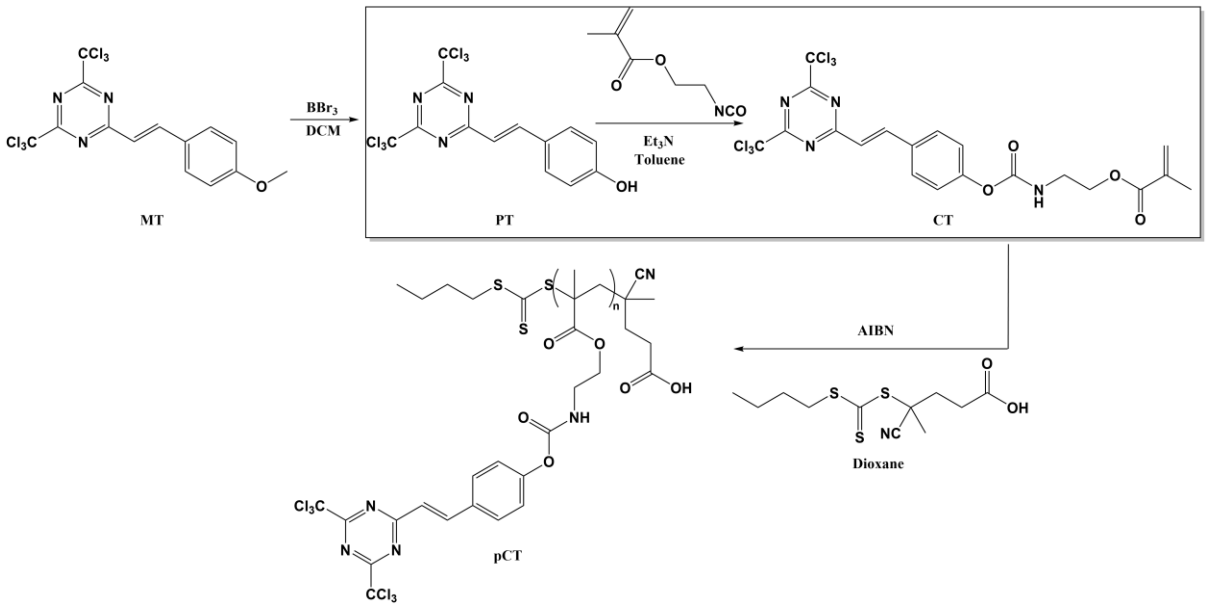

Scheme 2.1. Synthetic route for PT, CT, and pCT.

2.6 Results and discussion

2.6.1 Synthesis and characterization of triazine-derivatives

Triazine (MT) was first demethylated by BBr_3 to yield 4-(2-(4,6-Bis(trichloromethyl)-1,3,5-triazin-2-yl)vinyl)phenol (PT). PT was subsequently coupled with 2-isocyanatoethyl methacrylate to form polymerizable 2-(((4-(2-(4,6-bis(trichloromethyl)-1,3,5-triazin-2-yl)vinyl)phenoxy)carbonyl)amino)ethyl methacrylate (CT). Finally, CT was RAFT polymerized to yield a polymeric photoinitiator, pCT. The successful synthesis of CT was confirmed with ^{1}H NMR and ^{13}C NMR as shown in Figure 2.1. Specifically, H1, H4, and H5 proton signals in Figure 2.1a suggested the introduction of the methacrylate group, while the carbonyl group signal from C12 in Figure 2.1b indicated the formation of the carbamate.

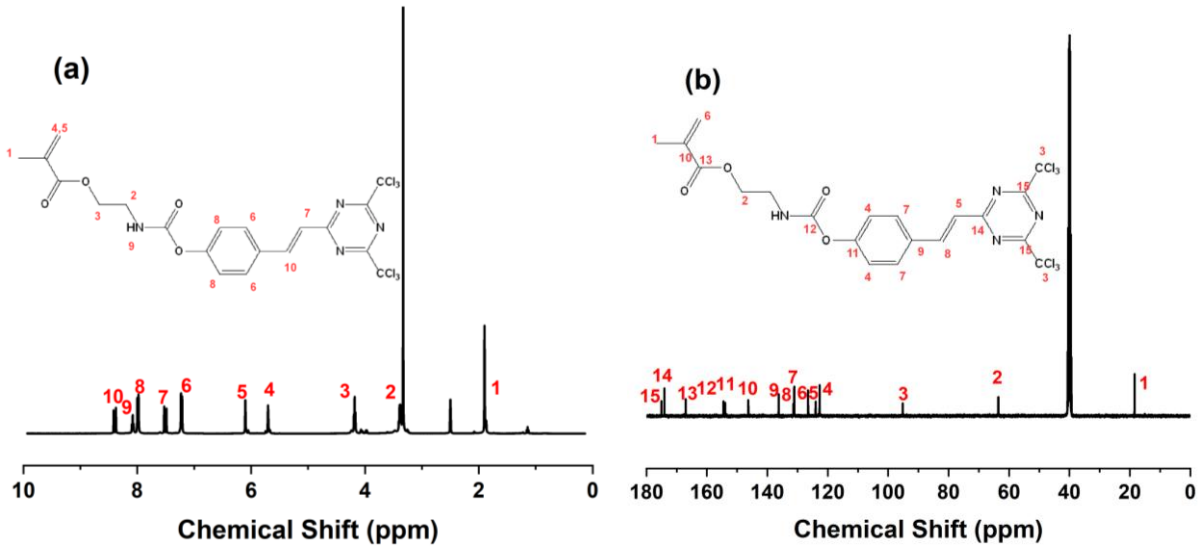

Figure 2.1. (a) ^{1}H NMR and (b) ^{13}C NMR spectra of CT in DMSO-d6 (400 MHz).

The prepared CT was also characterized using FTIR. As shown in Figure 2.2, the presence of the characterization bands at 3417 and 1703 cm^{-1} of CT attributed to the N-H and C=O stretching, respectively.[57] This again confirmed the successful synthesis of CT from PT. Finally, the RAFT polymerized CT (pCT) was examined to have M_n of 5240, M_w of 6840, and PDI of 1.305 using the GPC measurements (Figure 2.3). The triazine content of pCT was calculated via the equation: $MT\ wt\% = \frac{(M_n - M_{CPPA})}{M_n} \times \frac{M_{MT}}{M_{CT}} = 72\ wt\%$, where M_{CPPA}, M_{MT} and M_{CT} are molecular weight of CPPA, MT and CT respectively.

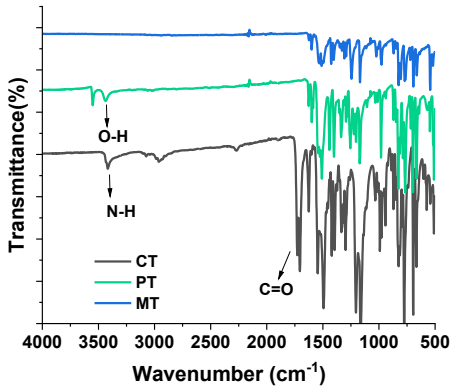

Figure 2.2. FTIR spectra of CT, PT, and MT.

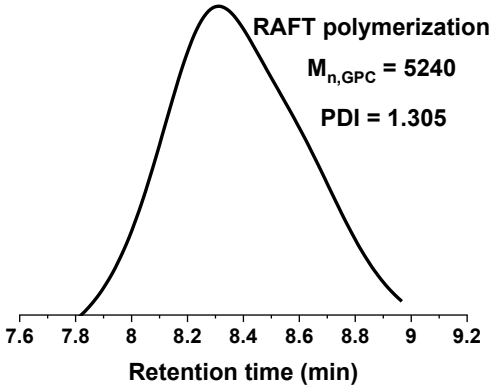

Figure 2.3. GPC elution profile of pCT synthesized by RAFT polymerization.

2.6.2 Light absorption properties of MT, PT, CT and pCT

The light absorption spectra of the investigated triazine derivatives in DMF are shown in Figure 2.4. To compare the light absorption properties of pCT with small molecule triazine derivatives, the equivalent concentration of triazine moiety of pCT was applied. Their light absorption maxima (λ_{max}) and extinction coefficients at the maximum absorption (ε_{max}) are summarized in Table 2.1. Compared to the maximum absorption peak of MT (λ_{max} = 380 nm), the maximum light absorption of PT is slightly red-shifted (λ_{max} = 385 nm), possibly due to the hydrogen bonding and the basic condition of DMF.[58] Specifically, phenol hydroxyl group of PT was involved in the hydrogen bonding with DMF, while the ionization of phenol hydroxyl group also led to the bathochromic shift. In contrast, those of CT and pCT were both blue-shifted (λ_{max} = 350 nm), which can be attributed to the fact that the substituents with low electron-donating abilities lead to the hypsochromic shift[59] The order of maximum absorption peak follows the order of electron-donating abilities: CT and pCT: -O(CO) < MT: -OMe < PT: -OH. Interestingly, even though the molar extinction coefficient of pCT (24900 M^{-1} cm^{-1}) is slightly lower than that of CT (29900 M^{-1} cm^{-1}), the light absorption of pCT is extended up to 460 nm (Figure 2.4). With the light absorption profiles of the synthesized triazine derivatives and the knowledge of the

photoinitiation mechanism[60], the following studies were performed under the irradiation of LED@400 nm or LED@410 nm (Table 2.1).

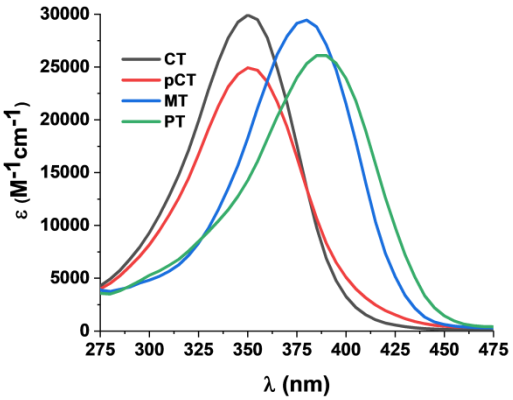

Figure 2.4. UV-vis absorption spectra of CT, pCT, MT, and PT in DMF.

Table 2.1. The maximum absorption wavelengths λmax, extinction coefficients ε_{max} at λ_{max} , $\varepsilon_{400\ nm}$ at 400 nm, and $\varepsilon_{410\ nm}$ at 410 nm of MT, PT, CT, and pCT in DMF.

Photoinitiators	λ_{max} (nm)	ε_{max} (M^{-1} cm^{-1})	$\varepsilon_{400\ nm}$ (M^{-1} cm^{-1})	$\varepsilon_{410\ nm}$ (M^{-1} cm^{-1})
MT	380	29400	21500	14000
PT	385	26000	23900	19000
CT	350	29900	3300	1500
pCT	350	24900	5100	3100

2.6.3 Photoinitiation abilities of triazine derivatives.

With the knowledge of the fact that the free radicals generated from the self-cleavage of MT are the active species for the initiation of the following polymerization of TMPTA[45], the photoinitiation ability of MT is efficient for the free radical polymerization of acrylates under the irradiation of LED@400 nm in terms of final double bond conversion (35.6%) and maximum rate of photopolymerization ($R_{p,max}$: 4.21 s^{-1}) (Figure 2.5a and Table 2.2). Furthermore, the higher intensity violet LED@410 nm (110 mW cm^{-2}) improves the photopolymerization of TMPTA in the presence of MT (Figure 2.5b), in line with the results reported previously.[43, 45, 53] To evaluate the effect of modification of MT structure on their photoinitiation abilities, the photopolymerization of TMPTA was carried out in laminate under both LED@400 nm

and LED@410 nm (Figure 2.5 and Table 2.2). The demethylated triazine derivative, PT showed similar final double bond conversions (36.2% and 46.4%) compared with MT (35.6% and 45.0%) (Table 2.2) upon exposure to LED@400 nm and LED@410 nm, respectively, but diminished $R_{p,max}$ to 3.31 s^{-1} and 7.34 s^{-1}. However, the polymerizable and the polymeric triazine derivatives, CT and pCT, exhibited reduced photoinitiation abilities in terms of both final double bond conversions and the $R_{p,max}$ to different extents (Figure 2.5 and Table 2.2). Specifically, CT and pCT reduced the final double bond conversions to 15.3% and 24.9% upon exposure to LED@400 nm, respectively (Table 2.2). This trend is in accordance with the discussed light absorption of the investigated triazine and its derivatives at 400 nm above, except for pCT (Table 2.1). As shown in Figure 2.5a, the overall slope of the TMPTA photopolymerization profile of pCT (red) revealed that the rate of polymerization was adversely affected by its nature as the polymeric photoinitiator. Specifically, the triazine moieties pendants on the chain of the polymethacrylate induced a huge steric effect which restricted the mobility of the generated free radicals, and hence significantly sacrificed the photoinitiation ability of corresponding photoinitiators.[61] Nevertheless, the slower polymerization rate in the pCT-based formula allowed the active species produced by pCT to release into the uncured resin gradually and resulted in a higher final double bond conversion of 24.9% compared to that produced by CT. In contrast, the $R_{p,max}$ of pCT is higher under LED@410 than under LED @400 nm (Table 2.2). This can be ascribed to the concentrated free radicals generated by pCT under LED@410 nm compared to that under LED@400 nm due to light intensity. Therefore, the distribution of active species in the uncured resin was promoted by the radical concentration gradient. The accelerated $R_{p,max}$ of pCT (2.97 s^{-1}) under LED@410 nm compared to LED@400 nm (0.18 s^{-1}) resulted in faster gelation of the monomers which the formed network subsequently reduced the mobility of residual active species and limited the diffusion of active species into the uncured sample, hence the final double bond conversion of TMPTA cannot reach a higher plateau. (Figure 2.5b).

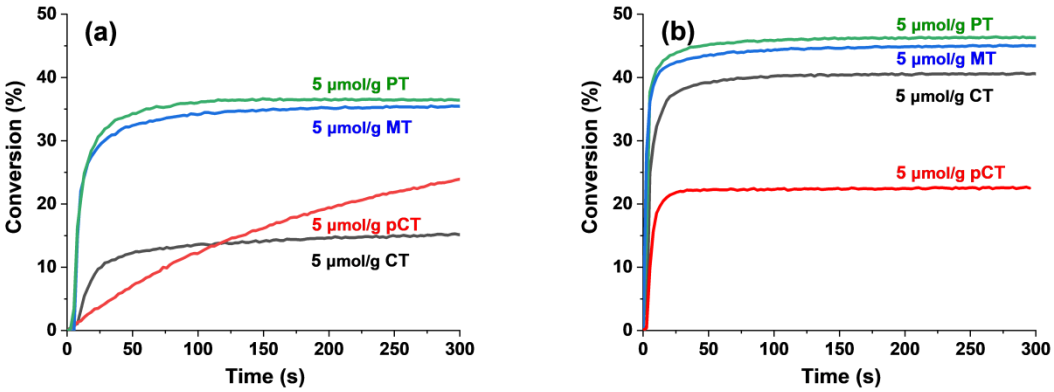

Figure 2.5. Photopolymerization profiles (double bond conversion vs time) of TMPTA obtained in laminate upon exposure to (a) LED@400 nm and (b) LED@410 nm in the presence of triazine derivative-based photoinitiators (molar concentrations of all triazine moieties are 5.0 μmol/g).

Table 2.2. Double bond conversions and polymerization rates of TMPTA in the presence of triazine derivatives (MT, PT, CT, and pCT) upon exposure to the LED@400 nm (6.4 mW cm^{-2}) and LED@410 nm (110 mW cm^{-2}) for 300 s.

Photoinitiators[a]	LED@400 nm		LED@410 nm	
	C[b]	(Rp/[C=C])×100[c]	C[b]	(Rp/[C=C])×100[c]
MT	35.6%	4.21 s^{-1}	45.0%	10.91 s^{-1}
PT	36.2%	3.31 s^{-1}	46.4%	7.34 s^{-1}
CT	15.3%	0.83 s^{-1}	40.5%	5.59 s^{-1}
pCT	24.9%	0.18 s^{-1}	22.5%	2.97 s^{-1}

[a] Contains equal molar concentration of the triazine moiety (5 μmol/g).
[b] Final double bond conversions of TMPTA after photopolymerization for 300 s.
[c] Maximum rates of photopolymerization, calculated from the maximum of the first derivative of the double bond conversions versus time curves during photopolymerization.

Additionally, the effect of light intensity and triazine moiety concentrations were investigated. As aforementioned, the increasing intensity of LED promoted the polymerization of TMPTA in the presence of identical photoinitiating systems in terms of both final double bond conversions and the $R_{p,max}$ (Table 2.2). Moreover, except for the 1.0 μmol/g pCT formulation, the increased amount of triazine moiety from 1.0 to 10.0 μmol/g resulted in the increased final double bond conversion for both pCT and CT under irradiation of LED@410 nm (Figure 2.6). The distinctive TMPTA photopolymerization profile of 1.0 μmol/g pCT (Figure 2.6a) is attributed to the aforementioned steric effect.

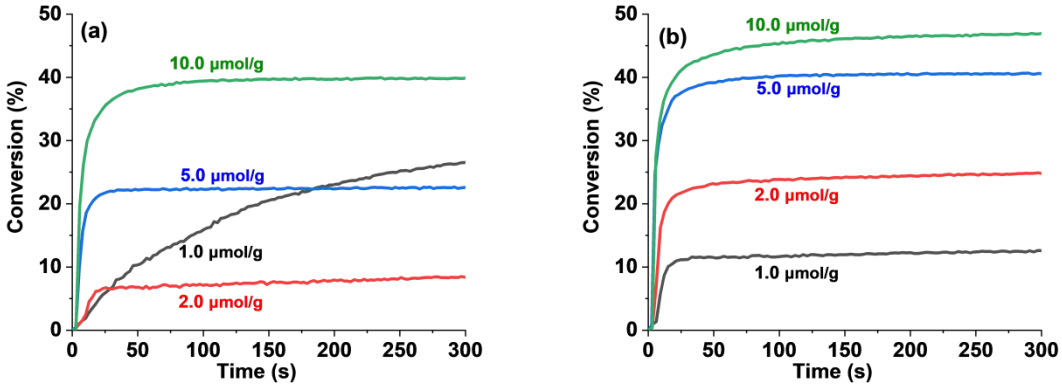

Figure 2.6. Photopolymerization profiles (double bond conversion vs time) of TMPTA obtained in laminate in the presence of diverse equivalent triazine moiety concentration (a) pCT and (b) CT upon exposure to LED@410 nm.

2.6.4 Migration of photoinitiators from photocured samples.

Residual photoinitiators and photolysis fragments tend to migrate to the surface of the photocured samples, which limits their application in biochemical materials.[19, 22-29] The migration stabilities of photocured samples (41.5 mg) were investigated by comparing the light absorption at the absorption maxima (λ_{max}) of each sample in their leaching solution (4 mL) as illustrated in Figure 2.7. Although the photoinitiation abilities of CT and pCT were reduced (Figure 2.5), their migration stabilities were significantly enhanced compared to MT (Table 2.3). Specifically, when irradiated by LED@400nm, PT showed the highest leachability (72.88%), possibly due to the strong hydrogen bonding interaction with solvent, which increased its solubility, while CT (13.35%) and pCT (2.88%) showed 1/3-fold and 1/14-fold leachability respectively compared to MT (41.03%). When irradiated by LED@410nm, the polymers were highlier crosslinked compared to that using LED@400 nm and thus the migration stabilities of all the samples were enhanced, especially for PT (11.91%) and MT (3.75%) but the trend remained the same as those with LED@400nm. Specifically, CT (1.55%) and pCT (0.61%) showed 1/2-fold and 1/6-fold leachability, respectively, compared to MT (3.75%).

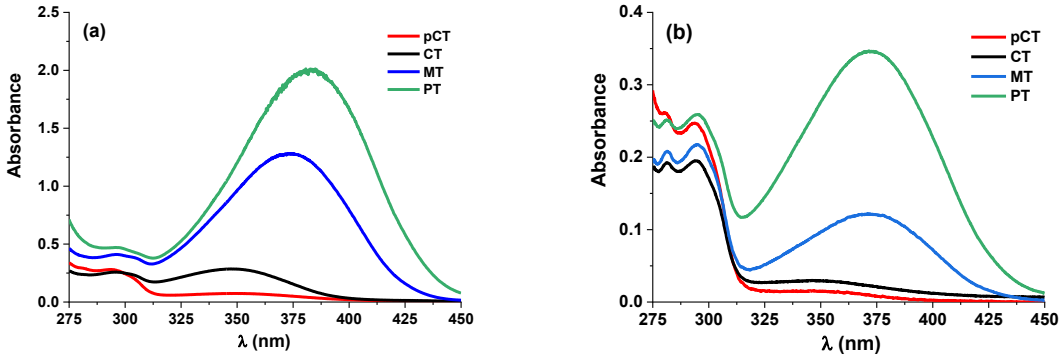

Figure 2.7. UV-vis absorption spectra of photoinitiators extracted with DMF for 20 h from the photopolymers prepared by the photopolymerization of TMPTA under the irradiation of (a) LED@400nm and (b) LED@410nm in the presence of 10.0 μmol/g triazine moiety of MT, PT, CT, and pCT in TMPTA.

Table 2.3. The migration ratio of photoinitiators from photocured samples.

Photoinitiators	LED@400 nm	LED@410 nm
MT	41.03%	3.75%
PT	72.88%	11.91%
CT	13.35%	1.55%
pCT	2.88%	0.61%

2.7 Materials and methods

2.7.1 Materials.

Unless specified, all chemicals were used as received. Trimethylolpropane triacrylate (TMPTA), 2-(4-methoxystyryl)-4,6-bis(trichloromethyl)-1,3,5-triazine (MT), boron tribromide (BBr_3, 1 M in heptane), dichloromethane (DCM; anhydrous), hexane, ethyl acetate (EA), absolute ethanol, toluene, triethylamine (TEA), azobisisobutyronitrile (AIBN), 2-isocyanatoethyl methacrylate, *N,N*-dimethylformamide (DMF), dimethylacetamide (DMA), acetonitrile (ACN), and dioxane were all purchased from Sigma-Aldrich. Deuterated dimethyl sulfoxide (DMSO-d_6) was obtained from Cambridge Isotope Laboratories, Andover, USA.

2.7.2 Synthesis.

2.7.2.1 4-(2-(4,6-Bis(trichloromethyl)-1,3,5-triazin-2-yl)vinyl)phenol (PT).

The synthesis of PT followed the literature.[43] Briefly, to the solution of 2-(4-methoxystyryl)-4,6- bis(trichloromethyl)-1,3,5-triazine (MT) (1 g, 2.2 mmol) in 100 mL of DCM at -78 °C, BBr_3 (60 mL, 1mol/L, 60 mmol) was added dropwise. The resultant mixture was allowed to warm to room temperature overnight and stirred for 1 day. The reaction mixture was then quenched by ice water (300 mL) and extracted by DCM. The organic layer was combined, dried with anhydrous sodium sulfate, and concentrated under vacuum, affording a yellow solid without further purification (780 mg, 80% yield).

2.7.2.2 Polymerizable 2-(((4-(2-(4,6-bis(trichloromethyl)-1,3,5-triazin-2-yl)vinyl)phenoxy)carbonyl)amino)ethyl methacrylate (CT).

To the solution of 4-(2-(4,6-Bis(trichloromethyl)-1,3,5-triazin-2-yl)vinyl)phenol (PT) (780 mg, 1.8 mmol) and TEA (0.5 ml, 3.6 mmol) in 20 ml toluene protected with N_2, the solution of 2-isocyanatoethyl methacrylate in 10 ml toluene was added. The resultant mixture was stirred at 60 °C for 18 h. The solvent was removed under vacuum, and the residue was purified by a silica column (10% EA/Hexane) to give a pale-yellow solid (700 mg, 66% yield).

^{1}H NMR (400 MHz, DMSO-d_6) δ 8.40 (d, J = 15.8 Hz, 1H), 8.08 (s, 1H), 7.99 (d, J = 8.6 Hz, 2H), 7.51 (d, J = 15.9 Hz, 1H), 7.22 (d, J = 8.5 Hz, 2H), 6.12 – 6.08 (m, 1H), 5.70 (t, J = 1.9 Hz, 1H), 4.18 (s, 2H), 3.39 (d, J = 5.6 Hz, 2H), 1.90 (s, 3H).

2.7.2.3 Polymerized 2-(((4-(2-(4,6-bis(trichloromethyl)-1,3,5-triazin-2-yl)vinyl)phenoxy)carbonyl)amino)ethyl methacrylate (pCT).

The RAFT reagent 4-cyano-4-(propylthiocarbonothioylthio)pentanoic acid (CPPA) was synthesized as previously reported.[62] CT (234 mg, 0.4 mmol), CPPA (5.5 mg, 0.02 mmol), and the thermal initiator AIBN (0.2 M, 55 μL, 0.01 mmol) were mixed in a

10 ml flask to make the ratio of [CT]:[CPPA]:[AIBN] to 20: 1: 0.5. The mixture with N_2 protection was degassed via freeze-pump-thaw cycles at least 3 times, and then heated to 60 °C and stirred for 10 h. The resulting polymer was purified with a short column to remove unpolymerized CT with (EA/DCM=10%), characterized by 1260 Agilent Infinity gel permeation chromatography (GPC) with DMA as the eluent.

2.7.3 Irradiation sources.

Two LEDs with different emission wavelengths and light intensities were used as irradiation devices for photopolymerization reactions: LEDs with emission wavelengths centered at 400 nm (6.4 mW cm^{-2}) and 410 nm (110 mW cm^{-2}).

2.7.4 Characterizations.

2.7.4.1 Infrared spectra

Spectra of MT, PT, and CT were acquired using a Spectrum Two Fourier transform infrared (FTIR) spectrometer (Perkin Elmer) fitted with attenuated total reflectance (ATR) accessory scans, with an average over the range of 500-4000 cm^{-1} at the resolution of 4 cm^{-1}.

2.7.4.2 Ultraviolet-Visible (UV-vis) Measurements

Ultraviolet-visible (UV-vis) measurements were conducted on a Varian Cary 50 Bio UV-vis spectrometer from Agilent Technologies, Malaysia.

2.7.4.3 Gel Permeation Chromatography Analysis

Gel permeation chromatography (GPC) eluent profile of pCT was characterized using a 1260 Agilent Infinity GPC at 30 °C, with DMA as the eluent and polystyrene as the standard.

2.7.4.4 NMR Spectroscopy

All the characterization experiments utilized AscendTM 400 MHz NMR from Bruker BioSpin AG, Fällanden, Switzerland. Chemical shifts were standardized using DMSO, δ = 2.50 ppm.

2.7.5 Photopolymerization Experiments

Photopolymerization of TMPTA in the presence of the investigated triazine-derived photoinitiators under the irradiation of LED at 400 nm (6.4 mW cm^{-2}) and 410 nm (100 mW cm^{-2}) was investigated using a real-time Fourier transform infrared spectroscopy INVENIO ® (RT-FTIR) manufactured by BRUKER. The free radical photopolymerization of TMPTA was conducted in laminate. Specifically, formulations were added in between two polypropylene films with a volume of samples of approximately 15 µL. The film was then sandwiched between two BaF_2 windows and placed on a measuring holder. The evolution of the double bond of TMPTA was at the band of 1620 cm^{-1}. Conversions of functional groups of monomers (C) during the photopolymerization processes were calculated via the equation: $C= (A_0-A_t)/A_0 \times 100\%$, where A_0 and A_t are the peak areas at the characterized band of TMPTA before irradiation and at time t irradiation, respectively.

2.7.6 Migration Test

The samples were prepared upon exposure to LED at 410 nm or LED at 400 nm in the presence of equal triazine moiety (10 µmol/g) with a thickness of 0.3 mm. The resultant samples were washed with ethanol to remove the unpolymerized monomer and immersed in DMF (4 mL) for 20 h. The leaching solution was measured using a UV-Vis spectrometer to determine the migration stability of the investigated photoinitiators. The calibration curves were plotted using their UV-Vis spectra with different equivalent concentrations of triazine moieties.

2.8 Conclusions

In summary, we prepared three triazine derivatives to investigate their photoinitiation abilities and migration stabilities. The blue-shifted light absorptions were found for the polymerizable and the RAFT polymerized triazine derivatives (CT and pCT), which reduced the photoinitiation abilities of both CT and pCT for the photopolymerization of TMPTA under the irradiation of LED at 400 nm compared to MT, while PT showed comparable photoinitiation efficiency to MT. In contrast, PT and CT kept comparable photoinitiation efficiency for the photopolymerization of TMPTA under the irradiation of LED at 410 nm compared to MT. Nevertheless, the migration stability of the photoinitiators was significantly enhanced in the photocured polymers photoinitiated by CT and pCT compared to that photoinitiated by MT under both LED at 400 nm and LED at 410 nm. Therefore, the discovery of the exceeding migration stabilities of CT and pCT can expand their applications in various areas, especially in the food packing or biochemical fields.

2.9 Supporting Information

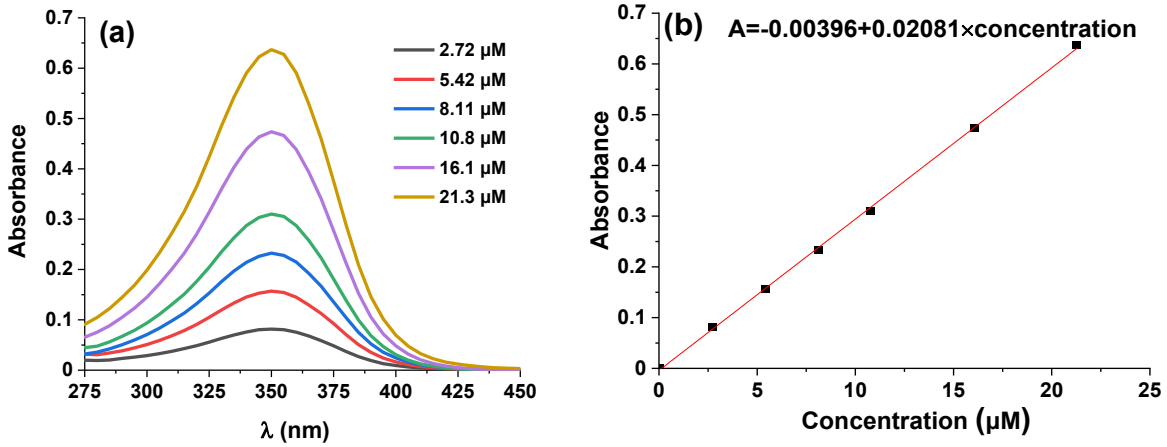

Figure S 2.1. (a) UV-vis spectra of different concentrations of CT and (b) calibration curve of CT (absorbance at 350 nm vs concentration) in DMF.

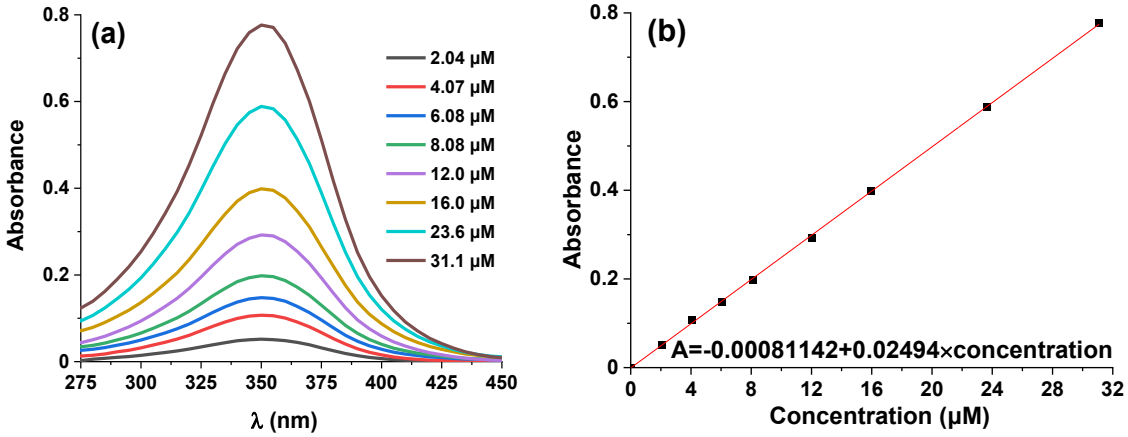

Figure S 2.2. (a) UV-vis spectra of pCT with different concentrations of triazine moiety and (b) calibration curve of triazine moiety (absorbance at 350 nm vs concentration of triazine moiety) in DMF.

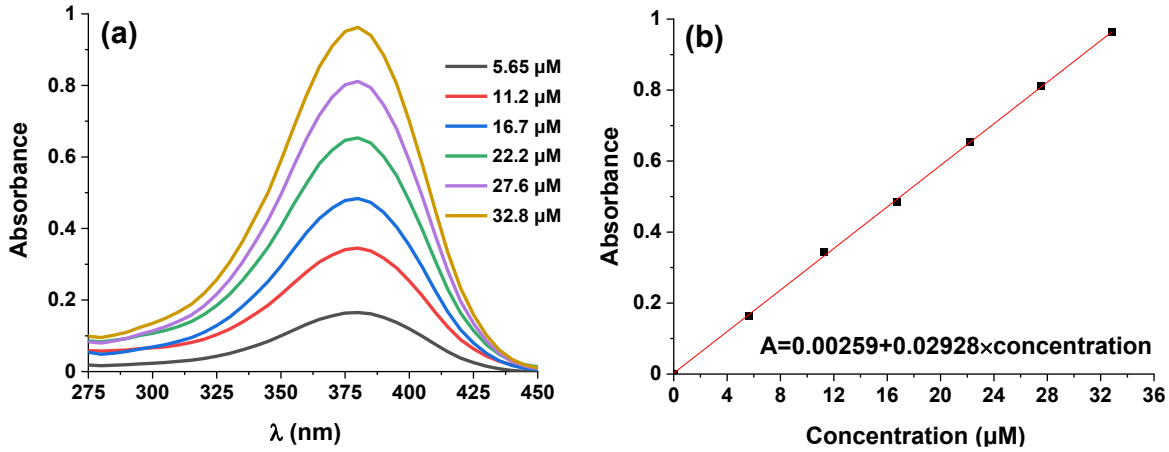

Figure S 2.3. (a) UV-vis spectra of different concentrations of MT and (b) calibration curve of MT (absorbance at 380 nm vs concentration) in DMF.

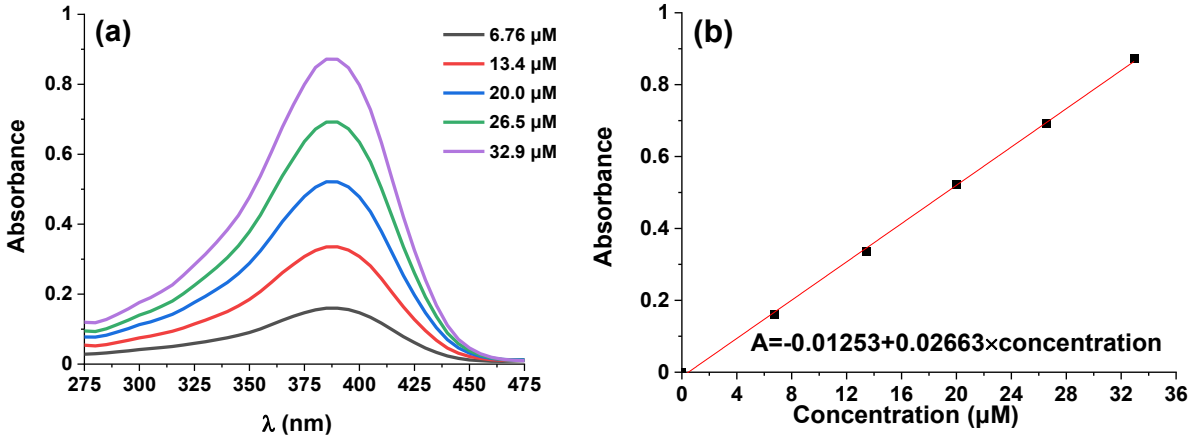

Figure S 2.4. (a) UV-vis spectra of different concentrations of PT and (b) calibration curve of PT (absorbance at 385 nm vs concentration) in DMF.

Migration concentration:

The migration concentration (c) was calculated based on the calibration curve of each photoinitiator as the function of absorbance (A).

CT: c = (A+0.00396)/ 0.02081

PT: c = (A+0.01253)/ 0.02663

MT: c = (A-0.00259)/ 0.02928

pCT: c = (A+0.00081142)/ 0.02494

Samples prepared under the irradiation of LED at 410 nm:

c_{PT} = 12.36 μM, c_{CT} = 1.61 μM, c_{MT} = 3.89 μM, c_{pCT} = 0.63 μM

Samples prepared under the irradiation of LED at 400 nm:

c_{PT} = 75.65 μM, c_{CT} = 13.86 μM, c_{MT} = 42.59 μM, c_{pCT} = 2.99 μM

Migration ratio:

The migration ratio (R) was calculated based on the formula

R = migration concentration/original concentration

Original concentration= triazine concentration × weight of sample/volume = 10 μmol/g×41.5 mg /4 mL= 103.8 μM

Samples prepared under the irradiation of LED at 410 nm:

R_{PT} = 11.91%, R_{CT} = 1.55%, R_{MT} = 3.75%, R_{pCT} = 0.61%

Samples prepared under the irradiation of LED at 400 nm:

R_{PT} = 72.88%, R_{CT} = 13.35%, R_{MT} = 41.03%, R_{pCT} = 2.88%

Table S 2.1. Migration concentrations of photoinitiators from the photocured samples in DMF.

Photoinitiators	LED at 400 nm	LED at 410 nm
MT (μM)	42.59	3.89
PT (μM)	75.65	12.36
CT (μM)	13.86	1.61
pCT (μM)	2.99	0.63

2.10 References

(1) Li, L.; Zhu, D.; Peng, X.; Xiao, P. Visible-Light-Sensitive Polymerizable and Polymeric Triazine-Based Photoinitiators with Enhanced Migration Stability. *Catalysts* **2022**, *12* (11), 1305.
(2) Xiao, P.; Zhang, J.; Dumur, F.; Tehfe, M. A.; Morlet-Savary, F.; Graff, B.; Gigmes, D.; Fouassier, J. P.; Lalevee, J. Visible light sensitive photoinitiating systems: Recent progress in cationic and radical photopolymerization reactions under soft conditions. *Prog. Polym. Sci.* **2015**, *41*, 32-66.
(3) Cataldi, A.; Corcione, C. E.; Frigione, M.; Pegoretti, A. Photocurable resin/nanocellulose composite coatings for wood protection. *Prog. Org. Coat.* **2017**, *106*, 128-136.
(4) Yagci, Y.; Jockusch, S.; Turro, N. J. Photoinitiated polymerization: advances, challenges, and opportunities. *Macromolecules* **2010**, *43* (15), 6245-6260.
(5) Leibfarth, F. A.; Mattson, K. M.; Fors, B. P.; Collins, H. A.; Hawker, C. J. External regulation of controlled polymerizations. *Angew. Chem. Int. Ed.* **2013**, *52* (1), 199-210.
(6) Liu, C.; Li, T.; Zhang, J.; Chen, S.; Xu, Z.; Zhang, A.; Zhang, D. Preparation and properties of phosphorous–nitrogen containing UV-curable polymeric coatings based on thiol–ene click reaction. *Prog. Org. Coat.* **2016**, *90*, 21-27.
(7) Chiulan, I.; Heggset, E. B.; Voicu, Ş. I.; Chinga-Carrasco, G. Photopolymerization of Bio-Based Polymers in a Biomedical Engineering Perspective. *Biomacromolecules* **2021**, *22* (5), 1795-1814.
(8) Wang, Z.; Guo, Y.; Cai, S.; Yang, J. Three-Dimensional Printing of Liquid Crystal Elastomers and Their Applications. *ACS Appl. Polym. Mater.* **2022**, *4* (5), 3153-3168.
(9) Ligon, S. C.; Liska, R.; Stampfl, J.; Gurr, M.; Mülhaupt, R. Polymers for 3D Printing and Customized Additive Manufacturing. *Chem. Rev.* **2017**, *117* (15), 10212-10290.
(10) Dietlin, C.; Schweizer, S.; Xiao, P.; Zhang, J.; Morlet-Savary, F.; Graff, B.; Fouassier, J.-P.; Lalevée, J. Photopolymerization upon LEDs: New photoinitiating systems and strategies. *Polym. Chem.* **2015**, *6* (21), 3895-3912.
(11) Anastasaki, A.; Nikolaou, V.; Zhang, Q.; Burns, J.; Samanta, S. R.; Waldron, C.; Haddleton, A. J.; McHale, R.; Fox, D.; Percec, V.; et al. Copper(II)/Tertiary Amine Synergy in Photoinduced Living Radical Polymerization: Accelerated Synthesis of ω-Functional and α,ω-Heterofunctional Poly(acrylates). *Journal of the American Chemical Society* **2014**, *136* (3), 1141-1149.
(12) Lee, E. K.; Park, C. H.; Lee, J.; Lee, H. R.; Yang, C.; Oh, J. H. Chemically robust ambipolar organic transistor array directly patterned by photolithography. *Adv. Mater.* **2017**, *29* (11), 1605282.
(13) Kütahya, C.; Wang, P.; Li, S.; Liu, S.; Li, J.; Chen, Z.; Strehmel, B. Carbon Dots as a Promising Green Photocatalyst for Free Radical and ATRP-Based Radical Photopolymerization with Blue LEDs. *Angew. Chem. Int. Ed.* **2020**, *59* (8), 3166-3171.
(14) Shanmugam, S.; Boyer, C. Organic photocatalysts for cleaner polymer synthesis. *Science* **2016**, *352* (6289), 1053-1054.
(15) Theriot, J. C.; Lim, C.-H.; Yang, H.; Ryan, M. D.; Musgrave, C. B.; Miyake, G. M. Organocatalyzed

atom transfer radical polymerization driven by visible light. *Science* **2016**, *352* (6289), 1082-1086.
(16) Liao, W.; Liao, Q.; Xu, C.; Wu, X.; Xiong, Y.; Li, Z.; Tang, H. Structural Effects of Cinnamoyl-Indanone-Based Photobleachable Free Radical Visible Initiators. *ACS Appl. Polym. Mater.* **2022**, *4* (9), 6466-6476.
(17) Chi, T.; Somers, P.; Wilcox, D. A.; Schuman, A. J.; Johnson, J. E.; Liang, Z.; Pan, L.; Xu, X.; Boudouris, B. W. Substituted Thioxanthone-Based Photoinitiators for Efficient Two-Photon Direct Laser Writing Polymerization with Two-Color Resolution. *ACS Appl. Polym. Mater.* **2021**, *3* (3), 1426-1435.
(18) Huang, X.; Zhang, Y.; Shi, M.; Zhang, Y.; Zhao, Y. Study on a polymerizable visible light initiator for fabrication of biosafety materials. *Polym. Chem.* **2019**, *10* (18), 2273-2281.
(19) Wu, Q.; Wang, X.; Xiong, Y.; Yang, J.; Tang, H. Thioxanthone based one-component polymerizable visible light photoinitiator for free radical polymerization. *RSC Adv.* **2016**, *6* (70), 66098-66107.
(20) Liska, R. Industrial Photoinitiators: A Technical Guide. by W. Arthur Green. *ChemPhysChem* **2011**, *12* (7), 1389-1389.
(21) Ay, E.; Raad, Z.; Dautel, O.; Dumur, F.; Wantz, G.; Gigmes, D.; Fouassier, J.-P.; Lalevée, J. Oligomeric Photocatalysts in Photoredox Catalysis: Toward High Performance and Low Migration Polymerization Photoinitiating Systems. *Macromolecules* **2016**, *49* (6), 2124-2134.
(22) Johns, S.; Jickells, S.; Read, W.; Castle, L. Studies on functional barriers to migration. 3. Components from cartonboard to food during frozen storage and microwave heating. *Packag Technol Sci* **2000**, *13*, 99-104.
(23) Papilloud, S.; Baudraz, D. Analysis of food packaging UV inks for chemicals with potential to migrate into food simulants. *Food Additives & Contaminants* **2002**, *19* (2), 168-175.
(24) Sanches-Silva, A.; Pastorelli, S.; Cruz, J.; Simoneau, C.; Castanheira, I.; Paseiro-Losada, P. Development of an analytical method for the determination of photoinitiators used for food packaging materials with potential to migrate into milk. *J. Dairy Sci.* **2008**, *91* (3), 900-909.
(25) Pastorelli, S.; Sanches-Silva, A.; Cruz, J. M.; Simoneau, C.; Losada, P. P. Study of the migration of benzophenone from printed paperboard packages to cakes through different plastic films. *Eur. Food Res. Technol.* **2008**, *227* (6), 1585-1590.
(26) Rodriguez-Bernaldo de Quiros, A.; Paseiro-Cerrato, R.; Pastorelli, S.; Koivikko, R.; Simoneau, C.; Paseiro-Losada, P. Migration of photoinitiators by gas phase into dry foods. *J. Agric. Food. Chem.* **2009**, *57* (21), 10211-10215.
(27) Sanches-Silva, A.; Andre, C.; Castanheira, I.; Cruz, J. M.; Pastorelli, S.; Simoneau, C.; Paseiro-Losada, P. Study of the migration of photoinitiators used in printed food-packaging materials into food simulants. *J. Agric. Food. Chem.* **2009**, *57* (20), 9516-9523.
(28) Shen, D.-x.; Lian, H.-z.; Ding, T.; Xu, J.-z.; Shen, C.-y. Determination of low-level ink photoinitiator residues in packaged milk by solid-phase extraction and LC-ESI/MS/MS using triple-quadrupole mass analyzer. *Analytical and bioanalytical chemistry* **2009**, *395* (7), 2359-2370.
(29) Qi, Y.; Zhang, X.; Huang, X.; Zhang, Y.; Shi, M.; Zhao, Y. High-efficient lignin-based polymerizable macromolecular photoinitiator with UV-blocking property for visible light polymerization. *Int. J. Biol. Macromol.* **2022**, *204*, 234-244.
(30) Xiao, P.; Dumur, F.; Frigoli, M.; Tehfe, M.-A.; Graff, B.; Fouassier, J. P.; Gigmes, D.; Lalevée, J. Naphthalimide based methacrylated photoinitiators in radical and cationic photopolymerization under visible light. *Polym. Chem.* **2013**, *4* (21), 5440-5448.
(31) Wei, J.; Wang, B. A Highly Efficient Polymerizable Photoinitiator Comprising Benzophenone, Thio Moieties, and N-Arylmaleimide. *Macromol. Chem. Phys.* **2011**, *212* (1), 88-95.
(32) Liang, S.; Yang, Y. D.; Zhou, H. Y.; Li, Y. Q.; Wang, J. X. Novel polymerizable HMPP-type photoinitiator with carbamate: Synthesis and photoinitiating behaviors. *Prog. Org. Coat.* **2017**, *110*, 128-133.
(33) Wang, J.; Yang, J.; Atif, M.; Bongiovanni, R.; Li, G.; Xue, Z.; Yang, X. One-component photoinitiator based on benzophenone and sesamol. *Polym. Adv. Technol.* **2018**, *29* (8), 2264-2272.
(34) Kreutzer, J.; Yagci, Y. One-component, double-chromophoric thioxanthone photoinitiators for free radical polymerization. *J. Polym. Sci., Part A: Polym. Chem.* **2017**, *55* (20), 3475-3482.
(35) Hutchison, J. B.; Stark, P. F.; Hawker, C. J.; Anseth, K. S. Polymerizable living free radical initiators as a platform to synthesize functional networks. *Chem. Mater.* **2005**, *17* (19), 4789-4797.
(36) Wang, J.; Stanic, S.; Altun, A. A.; Schwentenwein, M.; Dietliker, K.; Jin, L.; Stampfl, J.; Baudis, S.;

Liska, R.; Grützmacher, H. A highly efficient waterborne photoinitiator for visible-light-induced three-dimensional printing of hydrogels. *Chem. Commun.* **2018**, *54* (8), 920-923.
(37) Sandmeier, M.; Paunović, N.; Conti, R.; Hofmann, L.; Wang, J.; Luo, Z.; Masania, K.; Wu, N.; Kleger, N.; Coulter, F. B.; et al. Solvent-Free Three-Dimensional Printing of Biodegradable Elastomers Using Liquid Macrophotoinitiators. *Macromolecules* **2021**, *54* (17), 7830-7839.
(38) Deng, L.; Tang, L.; Qu, J. Synthesis and photopolymerization of novel UV-curable macro-photoinitiators. *Prog. Org. Coat.* **2020**, *141*, 105546.
(39) Yang, J.; Liao, W.; Xiong, Y.; Wang, X.; Li, Z.; Tang, H. A multifunctionalized macromolecular silicone-naphthalimide visible photoinitiator for free radical polymerization. *Prog. Org. Coat.* **2018**, *115*, 151-158.
(40) Gacal, B.; Akat, H.; Balta, D. K.; Arsu, N.; Yagci, Y. Synthesis and Characterization of Polymeric Thioxanthone Photoinitatiors via Double Click Reactions. *Macromolecules* **2008**, *41* (7), 2401-2405.
(41) Wang, C.; Venditti, R. A. UV Cross-Linkable Lignin Thermoplastic Graft Copolymers. *ACS Sustainable Chem. Eng.* **2015**, *3* (8), 1839-1845.
(42) Zhou, J.; Allonas, X.; Ibrahim, A.; Liu, X. Progress in the development of polymeric and multifunctional photoinitiators. *Prog. Polym. Sci.* **2019**, *99*, 101165.
(43) Peng, X.; Zhang, J.; Stachurski, Z. H.; Banaszak Holl, M. M.; Xiao, P. Visible-Light-Sensitive Triazine-Coated Silica Nanoparticles: A Dual Role Approach to Polymer Nanocomposite Materials with Enhanced Properties. *ACS Appl. Mater. Interfaces* **2021**, *13* (38), 46033-46042.
(44) Fan, Y.; Song, Y.; He, N.; Cheng, F.; Jiao, X.; Lai, G.; Hua, X.; Yang, X. High Efficiency and Low Migration Hyperbranched Silicone Contain Macrophotoinitiators for UV-Cured Transparent Coatings. *Polymers* **2020**, *12* (12), 3005.
(45) Zhang, J.; Xiao, P.; Morlet-Savary, F.; Graff, B.; Fouassier, J. P.; Lalevée, J. A known photoinitiator for a novel technology: 2-(4-methoxystyryl)-4,6-bis(trichloromethyl)-1,3,5-triazine for near UV or visible LED. *Polym. Chem.* **2014**, *5* (20), 6019-6026.
(46) Fouassier, J.-P.; Lalevée, J. *Photoinitiators for polymer synthesis: scope, reactivity, and efficiency, 1st ed*; John Wiley & Sons, 2012.
(47) Fouassier, J.-P. *Photoinitiation, photopolymerization, and photocuring: fundamentals and applications*; Hanser, 1995.
(48) Crivello, J. *Photoinitiators for free radical cationic and anionic photopolymerization*; 1998.
(49) Dietliker, K. A compilation of photoinitiators commercially available for UV today. 2002; SITA.
(50) Bagheri, A.; Jin, J. Photopolymerization in 3D Printing. *ACS Appl. Polym. Mater.* **2019**, *1* (4), 593-611.
(51) Ullrich, G.; Ganster, B.; Salz, U.; Moszner, N.; Liska, R. Photoinitiators with functional groups. IX. Hydrophilic bisacylphosphine oxides for acidic aqueous formulations. *J. Polym. Sci., Part A: Polym. Chem.* **2006**, *44* (5), 1686-1700.
(52) Benedikt, S.; Wang, J.; Markovic, M.; Moszner, N.; Dietliker, K.; Ovsianikov, A.; Grützmacher, H.; Liska, R. Highly efficient water-soluble visible light photoinitiators. *J. Polym. Sci., Part A: Polym. Chem.* **2016**, *54* (4), 473-479.
(53) Lai, H.; Zhu, D.; Xiao, P. Yellow triazine as an efficient photoinitiator for polymerization and 3D printing under LEDs. *Macromol. Chem. Phys.* **2019**, *220* (18), 1900315.
(54) Fairbanks, B. D.; Schwartz, M. P.; Bowman, C. N.; Anseth, K. S. Photoinitiated polymerization of PEG-diacrylate with lithium phenyl-2,4,6-trimethylbenzoylphosphinate: polymerization rate and cytocompatibility. *Biomaterials* **2009**, *30* (35), 6702-6707.
(55) Bryant, S. J.; Nuttelman, C. R.; Anseth, K. S. Cytocompatibility of UV and visible light photoinitiating systems on cultured NIH/3T3 fibroblasts in vitro. *Journal of Biomaterials Science, Polymer Edition* **2000**, *11* (5), 439-457.
(56) Yan, J.; Lai, H.; Zeng, B.; Wang, L.; Xing, F.; Xiao, P. Photoinduced free radical-releasing systems and their anticancer properties. *Photochemical & Photobiological Sciences* **2022**, *21* (8), 1405-1417.
(57) Coates, J. Interpretation of Infrared Spectra, A Practical Approach. In *Encyclopedia of Analytical Chemistry*, 2006.
(58) Antosiewicz, J. M.; Shugar, D. UV–Vis spectroscopy of tyrosine side-groups in studies of protein structure. Part 1: basic principles and properties of tyrosine chromophore. *Biophys. Rev.* **2016**, *8* (2), 151-161.
(59) Brown, R. D. Effects of Substituents on Ultra-violet Absorption Spectra. *Nature* **1952**, *169* (4294), 286-287.

(60) Fouassier, J. P. *Photoinitiation, Photopolymerization, and Photocuring: Fundamentals and Applications*; Carl Hanser Verlag GmbH & Co, 1995.
(61) Li, S.; Wu, F.; Li, M.; Wang, E. Host/guest complex of Me-β-CD/2,2-dimethoxy-2-phenyl acetophenone for initiation of aqueous photopolymerization: Kinetics and mechanism. *Polymer* **2005**, *46* (25), 11934-11939.
(62) Lai, H.; Zhu, D.; Peng, X.; Zhang, J.; Lalevée, J.; Xiao, P. N-Aryl glycines as versatile initiators for various polymerizations. *Polym. Chem.* **2021**, *12* (13), 1991-2000.

Chapter 5 Conclusion & Future Work

This thesis presents significant advancements in the design and application of triazine derivatives as multifunctional cleavage (Type I) photoinitiators, addressing the critical bottlenecks of conventional visible light initiation systems—including narrow absorption bandwidths, high migration-related toxicity risks, and limited material-level multifunctionality—through a progressive research strategy spanning fundamental molecular engineering, polymerizable functionalization, and functional nanomaterial integration.

The scientific foundation of this work is established in Chapter 1 through a comprehensive review of recent developments in Type I photoinitiators. By systematically comparing phosphorus, group 14, oxime ester, water-soluble, and two-photon photoinitiator systems, this chapter elucidates the relationships between molecular structure, photophysical behavior, and practical performance while identifying the key design challenges that form the conceptual basis for the molecular engineering strategies developed in the subsequent research chapters. In particular, it highlights the considerable potential of triazine-based photoinitiators alongside the remaining challenges associated with visible light activation, migration stability, and multifunctionality.

Building directly upon the challenge of photoinitiator migration and the associated safety concerns, Chapter 2 introduces a polymerizable triazine monomer and its corresponding polymeric derivative. These engineered systems maintain efficient photoinitiation under 410 nm LED irradiation while dramatically reducing photoinitiator migration, demonstrating that polymerizable and polymeric photoinitiator design represents an effective molecular strategy for concurrently preserving photoinitiation efficiency and improving material safety. This study

therefore expands the applicability of triazine photoinitiators to safety-critical sectors, including food packaging and biomedical materials.

To overcome the limited visible light absorption of conventional triazine photoinitiators, Chapter 3 develops an alternative synthetic strategy that extends the conjugation of the triazine framework, shifting the absorption onset to approximately 500 nm and enabling efficient photoinitiation under 410, 445, and 465 nm LED irradiation. The expanded π-conjugated architecture also exhibits a substantially enhanced two-photon absorption cross section, highlighting its potential for two-photon polymerization. Meanwhile, the incorporation of methacrylate functionalities effectively improves migration stability by enabling covalent immobilization within the polymer network. These findings not only broaden the structural diversity and application scope of triazine-based photoinitiators, but also demonstrate the feasibility of integrating visible light activation, high nonlinear optical performance, and migration resistance within a single molecular design strategy.

Moving beyond molecular structural engineering, Chapter 4 explores the integration of triazine photoinitiators with carbon dot nanoparticles. The resulting hybrid system exhibits excellent compatibility with industrial resins such as TMPTA while significantly enhancing photochemical performance through strong light absorption, accelerated photolysis, and improved photoinitiation efficiency, ultimately enabling high-fidelity 3D printing. Beyond their role in improving photopolymerization, the incorporated carbon dots remain as functional nanofillers within the cured polymer, reinforcing the crosslinked network while imparting photothermal stimulus-responsive behavior. This study demonstrates that functional nanomaterial integration provides a versatile strategy for simultaneously regulating photopolymerization kinetics, mechanical performance, and material functionality.

Collectively, these studies establish a systematic and multi-level design framework for triazine-based photoinitiators. Rather than representing isolated structural optimizations, the individual research chapters form a coherent progression that addresses the key limitations restricting the practical application of visible light

photoinitiators. Beginning with the improvement of migration stability through polymerizable immobilization, followed by the expansion of visible light absorption and nonlinear optical performance through molecular engineering, and culminating in multifunctional enhancement through nanomaterial hybridization, this thesis demonstrates that the performance limitations of current photoinitiators cannot be effectively addressed through optimization of a single molecular property alone. Instead, the results collectively highlight an integrated molecular design philosophy in which photophysical properties, photochemical reactivity, migration behavior, polymer compatibility, and post-curing material functionality are simultaneously considered within a unified molecular design framework. Together, these studies validate the structure–property relationships established in Chapter 1 and demonstrate how rational molecular engineering can be translated into multifunctional photoinitiator design. This integrated strategy not only broadens the structural diversity of triazine photoinitiators but also provides generalizable design principles for the development of next-generation multifunctional visible light Type I photoinitiators.

More broadly, this thesis illustrates how rational molecular design can be translated from fundamental photochemistry into advanced photopolymerization technologies, including visible light curing, two-photon polymerization, and DLP 3D printing. Beyond the specific triazine derivatives reported herein, the design concepts established through polymerizable functionalization, conjugation engineering, and nanomaterial hybridization provide a versatile framework for developing multifunctional photoinitiators that satisfy the increasingly demanding requirements for efficiency, safety, processability, and material performance.

Despite these advances, several important challenges remain to define the frontiers of future research. The inherently limited water solubility of triazine derivatives restricts their application in aqueous formulations and hydrogel-based systems, requiring the future introduction of hydrophilic or ionic functionalities that do not compromise photoinitiation efficiency or migration stability. Furthermore, the intrinsic

trade-off between strong light absorption and deep light penetration continues to limit curing performance in thick or highly scattering materials. Overcoming this bottleneck requires advanced approaches, such as absorption tuning, dual-wavelength initiation, energy-transfer systems, and photobleaching strategies that allow deeper light propagation for hydrogel 3D printing, dental restorations, and multilayer coatings. Beyond depth and solubility constraints, extending triazine photoinitiators toward gradient or stimulus-responsive materials offers promising opportunities for creating spatially programmable mechanical properties mimicking natural tissues. Finally, as these materials move closer to practical implementation, systematic investigations into long-term biocompatibility, migration behavior under realistic service conditions, and environmental sustainability will be essential for facilitating their translation into industrial and biomedical applications.

Ultimately, future research must move beyond optimizing individual performance metrics and instead embrace the integrated regulation of molecular structure, photophysical behavior, polymer compatibility, and material functionality. Continued progress along these directions is expected to further expand the applicability of triazine-based photoinitiators and accelerate the development of next-generation multifunctional Type I photoinitiators for advanced industrial manufacturing and precision biomedical photopolymerization technologies.